arXiv:hep-ph/9904246v2 8 Sep 1999

Testing Nucleation Theory in Two Dimensions

Alessandro Strumia

Dipartimento di Fisica, Università di Pisa and
INFN, Sezione di Pisa, I-56127 Pisa, Italia

and

Nikolaos Tetradis

Scuola Normale Superiore,
Piazza dei Cavalieri 7, I-56126 Pisa, Italia

Abstract

We calculate bubble-nucleation rates for (2+1)-dimensional scalar theories at high temperature. Our approach is based on the notion of a real coarse-grained potential. The region of applicability of our method is determined through internal consistency criteria. We compare our results with data from lattice simulations. Good agreement is observed when the renormalized action of the simulated theory is known.

1 Introduction

1.1 The standard formalism

The standard formalism for the calculation of bubble-nucleation rates during first-order phase transitions in field theories at non-zero temperature was introduced in refs. [1]–[4]. It consists of an implementation of Langer's theory of homogeneous nucleation [5] (for a review see ref. [6]) within the field-theoretical context. The nucleation rate I gives the probability per unit time and volume to nucleate a certain region of the stable phase (the true vacuum) within the metastable phase (the false vacuum). Its calculation relies on a semiclassical approximation around a dominant saddle-point, which is identified with the critical bubble. This is a static configuration (usually assumed to be spherically symmetric) within the metastable phase whose interior consists of the stable phase. It has a certain radius that can be determined from the parameters of the underlying theory. Bubbles slightly larger than the critical one expand rapidly, thus converting the metastable phase into the stable one. The nucleation rate is exponentially suppressed by the action (the free energy rescaled by the temperature) of the critical bubble. Possible deformations of the critical bubble generate a pre-exponential factor. The leading contribution to this factor has the form of a ratio of fluctuation determinants and corresponds to the first-order correction to the semiclassical result in a systematic expansion around the saddle point.

For a $(d+1)$-dimensional theory of a real scalar field at temperature T, in the limit that thermal fluctuations dominate over quantum fluctuations, the bubble-nucleation rate is given by [2]–[4]

$$I = \frac{E_0}{2\pi}\left(\frac{S}{2\pi}\right)^{d/2}\left|\frac{\det'[\delta^2\Gamma/\delta\phi^2]_{\phi=\phi_{\mathrm{b}}}}{\det[\delta^2\Gamma/\delta\phi^2]_{\phi=0}}\right|^{-1/2}\exp\left(-S\right). \tag{1.1}$$

Here Γ is the free energy of the system for a given configuration of the field ϕ. The rescaled free energy of the critical bubble is $S = \Gamma_b/T = [\Gamma\left(\phi_{\mathrm{b}}(r)\right) - \Gamma(0)]/T$, where $\phi_{\mathrm{b}}(r)$ is the spherically-symmetric bubble configuration and $\phi = 0$ corresponds to the false vacuum. The prime in the fluctuation determinant around the bubble denotes that the d zero eigenvalues of the operator $[\delta^2\Gamma/\delta\phi^2]_{\phi=\phi_{\mathrm{b}}}$, corresponding to displacements of the bubble, have been removed. Their contribution generates the factor $(S/2\pi)^{d/2}$ and the volume factor that is absorbed in the definition of I (nucleation rate per unit volume). The quantity E_0 is the square root of the absolute value of the unique negative eigenvalue.

In field theory, the free energy density Γ of a system for homogeneous configurations is usually identified with the temperature-dependent effective potential. This is evaluated through some perturbative scheme, such as the loop expansion. The profile and the free energy of the critical bubble are determined through the potential. This approach, however, faces fundamental difficulties: For example, the effective potential, being the Legendre transform of the generating functional for the connected Green functions, is a convex function of the field. Consequently, it does not seem to be the appropriate quantity for the study of tunnelling. Also, the fluctuation determinants in the expression for the nucleation rate have a form completely analogous to the one-loop correction to the potential. The question of double-counting the effect of fluctuations (in the potential and the prefactor) must be properly addressed. A closely related issue concerns the ultraviolet divergences that are inherent in the calculation of the fluctuation determinants in the prefactor. An appropriate regularization scheme must be employed in order to control them [7]. Moreover, this scheme must be consistent with the one employed for the absorption of the divergences appearing in the calculation of the potential.

1.2 Coarse-graining

In refs. [8]–[11] it was shown that all the above issues can be resolved through the implementation of the notion of coarse graining in the formalism. The appropriate quantity for the description of the physical system is the effective average action Γ_k [12], which is the generalization in the continuum of the blockspin action of Kadanoff [13]. It can be interpreted as a coarse-grained free energy at a given scale k. Fluctuations with characteristic momenta $q^2 \gtrsim k^2$ are integrated out and their effect is incorporated in Γ_k. In the limit $k \to 0$, Γ_k becomes equal to the effective action. The k dependence of

Γ_k is described by an exact flow equation [14], typical of the Wilson approach to the renormalization group [15]. This flow equation can be translated into evolution equations for the functions appearing in a derivative expansion of the action [16, 17]. Usually, one considers only the effective average potential U_k and a standard kinetic term, and neglects higher derivative terms in the action. We shall employ this approximation in this paper also. The bare theory is defined at some high scale Λ that can be identified with the ultraviolet cutoff. At scales k below the temperature T, a $(d+1)$-dimensional theory at non-zero temperature can be described in terms of an effective d-dimensional action at zero temperature [18].

In ref. [9] we considered a $(3+1)$-dimensional theory of a real scalar field at non-zero temperature, defined through its action Γ_{k_0} at a scale k_0 below the temperature, so that the theory has an effective three-dimensional description. The form of the potential U_{k_0} results from the bare potential U_Λ after the integration of (quantum and thermal) fluctuations between the scales Λ and k_0. We computed the form of the U_k at scales $k \leq k_0$ by integrating an evolution equation derived from the exact flow equation for Γ_k. U_k is non-convex for non-zero k, and approaches convexity only in the limit $k \to 0$. The nucleation rate must be computed for k larger than the scale k_f at which the functional integral in the definition of U_k starts receiving contributions from field configurations that interpolate between the two minima. This happens when $-k^2$ becomes approximately equal to the negative curvature at the top of the barrier [19]. For $k \gtrsim k_f$ the typical length scale of a thick-wall critical bubble is $\gtrsim 1/k$. We performed the calculation of the nucleation rate for a range of scales above and near k_f, for which U_k is non-convex. In our approach the pre-exponential factor is well-defined and finite, as an ultraviolet cutoff of order k is implemented in the calculation of the fluctuation determinants, so that fluctuations with characteristic momenta $q^2 \gtrsim k^2$ are not included. This is a natural consequence of the fact that all fluctuations with typical momenta above k are already incorporated in the form of U_k. This modification also resolves naturally the problem of double-counting the effect of the fluctuations.

We found that the saddle-point configuration has an action S_k with a significant k dependence. For strongly first-order phase transitions, the nucleation rate $I = A_k \exp(-S_k)$ is dominated by the exponential suppression. The main role of the prefactor A_k, which is also k dependent, is to remove the scale dependence from the total nucleation rate. Thus, this physical quantity is independent of the scale k that we introduced as a calculational tool. The implication of our results is that the critical bubble should not be identified just with the saddle point of the semiclassical approximation. It is the combination of the saddle point and its possible deformations in the thermal bath (accounted for by the fluctuation determinant in the prefactor) that has physical meaning. We also found that, for progressively more weakly first-order phase transitions, the difference between S_k and $\ln(A_k/k_f^4)$ diminishes. This indicates that the effects of fluctuations become more enhanced. At the same time, a significant k dependence of the predicted nucleation rate develops. The reason for the above deficiency is clear. When the nucleation rate is roughly equal to or smaller than the contribution from the prefactor, the effect of the next order in the expansion around the saddle point is important and can no longer be neglected. This indicates that there is a limit to the validity of Langer's picture of homogeneous nucleation. The region of validity of this picture was investigated in detail in ref. [10]. First-order phase transitions in two-scalar models were studied in ref. [11] and the consistency of the approach summarized above was reconfirmed. Moreover, the applicability of homogeneous nucleation theory to radiatively-induced first-order phase transitions was tested. It was found that the expansion around the semiclassical saddle point is not convergent for such phase transitions. This indicates that estimates of bubble-nucleation rates for the electroweak phase transition that are based only on the saddle-point action may be very misleading.

1.3 Plan of the paper

In this paper we present an application of our formalism to $(2+1)$-dimensional theories at non-zero temperature. Our investigation provides a new test of several points of our approach that depend strongly on the dimensionality, such as the form of the evolution equation of the potential, the nature of the ultraviolet divergences of the fluctuation determinants, and the k dependence of the saddle-point action and prefactor. The complementarity between the k dependence of S_k and A_k is a crucial

requirement for the nucleation rate I to be k independent. A strong motivation for this study stems from the existence of lattice simulations of nucleation for (1+1) and (2+1)-dimensional systems [20, 21]. In particular, we shall compare our predictions for the nucleation rate with the lattice results of ref. [21].

In the next section we summarize the basic steps of our method and derive the necessary expressions for the calculation of the nucleation rate. In section 3 we present sample calculations in two dimensions. In section 4 we apply our formalism to theories that have been studied through lattice simulations and compare with the lattice results. Our conclusions are presented in section 5.

2 The calculation of bubble-nucleation rates

2.1 Evolution equation for the potential

We consider a model of a real scalar field ϕ in 2+1 dimensions. The effective average action $\Gamma_k(\phi)$ [12] is obtained by adding an infrared cutoff term to the bare action, so that contributions from modes with characteristic momenta $q^2 \lesssim k^2$ are not taken into account. We use the simplest choice of a mass-like cutoff term $\sim k^2\phi^2$, for which the perturbative inverse propagator for massless fields is $P_k(q) \sim q^2 + k^2$. This choice makes the calculation of the fluctuation determinants in the pre-exponential factor of the nucleation rate technically feasible. Subsequently, the generating functional for the connected Green functions is defined, from which the generating functional for the 1PI Green functions can be obtained through a Legendre transformation. The presence of the modified propagator in the above definitions results in the effective integration of the fluctuations with $q^2 \gtrsim k^2$ only. Finally, the effective average action is obtained by removing the infrared cutoff from the generating functional for the 1PI Green functions.

The effective average action Γ_k obeys an exact flow equation, which describes its response to variations of the infrared cutoff k [14]. This can be turned into evolution equations for the functions appearing in a derivative expansion of Γ_k [16]. In this work we use an approximation which neglects higher derivative terms in the action and approximates it by

$$\Gamma_k = \int d^2x \left\{ \frac{1}{2}\partial^\mu\phi \, \partial_\mu\phi \; + U_k(\phi) \right\}. \tag{2.1}$$

The above action describes the effective two-dimensional theory that results from the dimensional reduction of a high-temperature (2+1)-dimensional theory at scales below the temperature. The temperature has been absorbed in a redefinition of the fields and their potential, so that these have dimensions appropriate for an effective two-dimensional theory. The correspondence between the quantities we use and the ones of the (2+1)-dimensional theory is given by

$$\phi = \frac{\phi_{2+1}}{\sqrt{T}}, \qquad U(\phi) = \frac{U_{2+1}\left(\phi_{2+1}, T\right)}{T}. \tag{2.2}$$

In this way, the temperature does not appear explicitly in our expressions. This has the additional advantage of permitting the straightforward application of our results to the problem of quantum tunnelling in a two-dimensional theory at zero temperature [9].

The evolution equation for the potential can be written in the form [14, 16, 10]

$$\frac{\partial}{\partial k^2}\left[U_k(\phi) - U_k(0)\right] = -\frac{1}{8\pi}\left[\ln\left(1 + \frac{U_k''(\phi)}{k^2}\right) - \ln\left(1 + \frac{U_k''(0)}{k^2}\right)\right]. \tag{2.3}$$

For the numerical integration of the above equation we use the algorithms described in ref. [23]. The first step of an iterative solution of eq. (2.3) gives [22]

$$U_k^{(1)}(\phi) - U_k^{(1)}(0) = U_{k_0}(\phi) - U_{k_0}(0) + \frac{1}{2}\ln\left[\frac{\det[-\partial^2 + k^2 + U_{k_1}''(\phi)]}{\det[-\partial^2 + k_0^2 + U_{k_1}''(\phi)]}\frac{\det[-\partial^2 + k_0^2 + U_{k_1}''(0)]}{\det[-\partial^2 + k^2 + U_{k_1}''(0)]}\right]. \tag{2.4}$$

The scale k_1 in the above expression can be chosen arbitrarily anywhere between k_0 and k, as the induced uncertainty for $U_k^{(1)}(\phi)$ corresponds to a higher-order contribution in the iterative procedure.

For $k_1 = k_0$, $k \to 0$, eq. (2.4) is a regularized one-loop approximation to the effective potential. Due to the ratio of determinants, only momentum modes with $k^2 \lesssim q^2 \lesssim k_0^2$ are effectively included in the momentum integrals. The above expression demonstrates the form of ultraviolet regularization of fluctuation determinants that is consistent with the cutoff procedure that leads to the evolution equation for the potential. An analogous regularization must be used for the fluctuation determinants in the expression for the nucleation rate.

2.2 The nucleation rate

The calculation of the nucleation rate proceeds in complete analogy to the one in ref. [9] which we outlined in the introduction. We define the theory through the potential at a scale k_0 below the temperature, so that the behaviour is effectively two-dimensional. We then integrate the evolution equation down to a scale $k \gtrsim k_f$, where we compute the bubble-nucleation rate. In practice, k_f^2 is taken 10% larger than the absolute value of the curvature at the top of the barrier. The potential has two minima: the stable (true) one located at $\phi = \phi_t$, and the unstable (false) one at $\phi = \phi_f = 0$. The nucleation rate is exponentially suppressed by the action S_k (the free energy rescaled by the temperature) of the saddle-point configuration $\phi_b(r)$ that is associated with tunnelling. This is an $SO(2)$-symmetric solution of the classical equations of motion which interpolates between the local maxima of the potential $-U_k(\phi)$. It satisfies the equation

$$\frac{d^2\phi_b}{dr^2} + \frac{1}{r}\frac{d\phi_b}{dr} = U_k'(\phi_b), \tag{2.5}$$

with the boundary conditions $\phi_b \to 0$ for $r \to \infty$ and $d\phi_b/dr = 0$ for $r = 0$. The action S_k of the saddle point is given by

$$S_k = 2\pi \int_0^\infty \left[\frac{1}{2}\left(\frac{d\phi_b(r)}{dr}\right)^2 + U_k(\phi_b(r)) - U_k(0)\right] r\, dr \equiv S_k^t + S_k^v. \tag{2.6}$$

The profile of the saddle point can be easily computed with the "shooting" method [24]. A consistency check for our solution is provided by the fact that $S_k^v = 0$ for two-dimensional theories.

The bubble-nucleation rate is determined through eq. (1.1) in terms of the potential $U_k(\phi)$. The explicit temperature dependence is absorbed in the definition of effective two-dimensional parameters according to eq. (2.2). An appropriate regularization is implemented in order to control the ultraviolet divergence of the prefactor. The type of regularization is dictated by the one-loop effective potential, given by eq. (2.4) in our scheme. This equation indicates that fluctuation determinants computed within the low-energy theory must be replaced by appropriate ratios of determinants. We emphasize that the matching of the regularization scheme for the prefactor with the cutoff used for the derivation of the evolution equation for the potential (2.3) is crucial for the consistency of our method. Finally, the nucleation rate in two dimensions is given by

$$I = A_k \exp(-S_k)$$

where

$$A_k = \frac{E_0}{2\pi}\frac{S_k}{2\pi}\left|\frac{\det'\left[-\partial^2 + U_k''(\phi_b(r))\right]}{\det\left[-\partial^2 + k^2 + U_k''(\phi_b(r))\right]}\frac{\det\left[-\partial^2 + k^2 + U_k''(0)\right]}{\det\left[-\partial^2 + U_k''(0)\right]}\right|^{-1/2}. \tag{2.7}$$

The differential operators that appear in eq. (2.7) have the general form

$$\mathcal{W}_{\kappa\alpha} = -\partial^2 + m_\kappa^2 + \alpha W_k(r) \tag{2.8a}$$

where

$$m_\kappa^2 \equiv U_k''(0) + \kappa k^2, \tag{2.8b}$$
$$W_k(r) \equiv U_k''(\phi_b(r)) - U_k''(0), \tag{2.8c}$$

4

with $\kappa, \alpha = 0$ or 1. As the $\mathcal{W}_{\kappa\alpha}$ operators are $SO(2)$-symmetric, it is convenient to use polar coordinates and express their eigenfunctions as $\psi_n(r, \varphi) = e^{in\varphi} u_n(r)/\sqrt{r}$. This leads to

$$\det \mathcal{W}_{\kappa\alpha} = \prod_{n=-\infty}^{\infty} \det \mathcal{W}_{n\kappa\alpha}$$

$$\mathcal{W}_{n\kappa\alpha} = -\frac{d^2}{dr^2} + \frac{n^2 - \frac{1}{4}}{r^2} + m_\kappa^2 + \alpha W_k(r). \tag{2.9}$$

The computation of such determinants is made possible by a theorem [25] that relates ratios of determinants to solutions of ordinary differential equations. In particular, we have

$$g_{n\kappa} \equiv \frac{\det \mathcal{W}_{n\kappa1}}{\det \mathcal{W}_{n\kappa0}} = \frac{y_{n\kappa1}(r \to \infty)}{y_{n\kappa0}(r \to \infty)}, \tag{2.10}$$

where $y_{n\kappa\alpha}(r)$ is the solution of the differential equation

$$\left[-\frac{d^2}{dr^2} + \frac{n^2 - \frac{1}{4}}{r^2} + m_\kappa^2 + \alpha W_k(r) \right] y_{n\kappa\alpha}(r) = 0, \tag{2.11}$$

with the behaviour $y_{n\kappa\alpha}(r) \propto r^{|n|+\frac{1}{2}}$ for $r \to 0$. For example, $y_{n\kappa0}$ are proportional to modified Bessel functions: $y_{n\kappa0} \propto \sqrt{r}\, I_{|n|}(m_\kappa r)$. Equations such as (2.11) can be solved numerically with Mathematica [26]. Since opposite values of n lead to identical determinants, the final expression for the nucleation rate can be written as

$$I = \frac{1}{2\pi} \left(\frac{S_k}{2\pi} \right) \exp(-S_k) \prod_{n=0}^{\infty} c_n,$$

$$c_0 = \left(\frac{E_0^2 g_{01}}{|g_{00}|} \right)^{1/2}, \qquad c_1 = \frac{g_{11}}{g'_{10}}, \qquad c_n = \frac{g_{n1}}{g_{n0}}. \tag{2.12}$$

The calculation of c_1 is slightly complicated because of the necessity to eliminate the zero eigenvalue in g'_{10}. (The two zero eigenvalues of the operator $-\partial^2 + U_k''(\phi_b(r))$ are included in the equal factors g_{-10} and g_{10}). Also the (unique) negative eigenvalue $-E_0^2$ must be computed for the determination of c_0. How these steps are achieved is described in ref. [9]. For sufficiently large n, one can compute c_n analytically using first-order perturbation theory in $W_k(r)$ [7, 9]. We find

$$g_{n\kappa} \approx 1 + \frac{1}{2n} \int r\, W_k(r)\, dr, \qquad c_n \approx 1 - \frac{1}{4n^3} k^2 \int r^3\, W_k(r)\, dr. \tag{2.13}$$

These expressions are very useful for the evaluation of the prefactor, as only c_n for small values of n need to be computed numerically.

3   A sample computation

We are interested in potentials that have the approximate form

$$V(\phi) = \frac{m^2}{2} \phi^2 + \frac{\gamma}{6} \phi^3 + \frac{h}{8} \phi^4. \tag{3.1}$$

The explicit temperature dependence has been absorbed in γ, h and ϕ according to eqs. (2.2). Through a shift $\phi \to \phi + c$ the cubic term in eq. (3.1) can be eliminated in favour of a term linear in ϕ. The resulting potential describes a statistical system of the Ising universality class in the presence of an external magnetic field. We assume that the potential of eq. (3.1) describes the theory at some initial scale k_0 not far below the temperature, similarly to refs. [9]–[11]. Its form at lower scales can
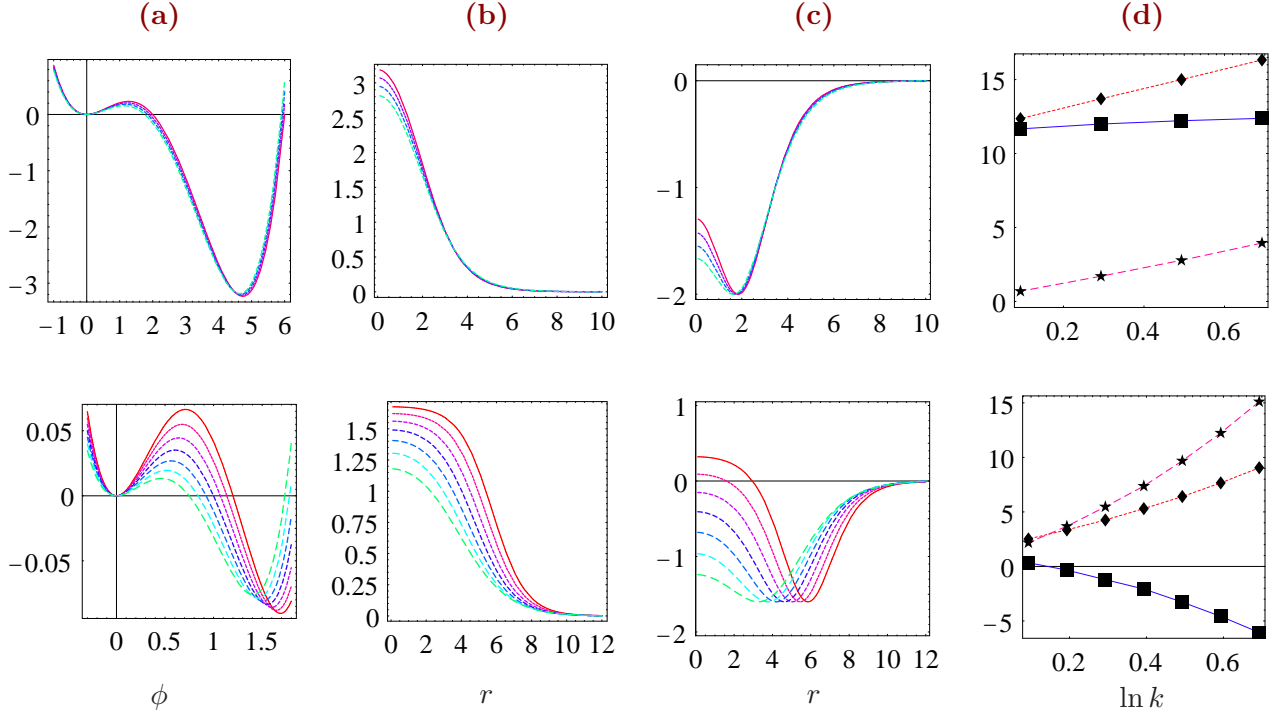
Figure 1: *The steps in the computation of the nucleation rate:* (a) *Potentials $V_k(\phi)$;* (b) *Saddle points $\phi_b(r)$;* (c) *$W_k(r)$, given by eq. (2.8c);* (d) *Results for the saddle-point action S_k (diamonds), prefactor $\ln\left(A_k/m^3\right)$ (stars) and nucleation rate $-\ln\left(I/m^3\right)$ (squares). The first row corresponds to a model with a potential $U_{k_0}(\phi)$ given by eq. (3.1) with $\gamma/m^2 = -2$, $h/m^2 = 1/3$, while the second one to a model with $\gamma/m^2 = -4.5$, $h/m^2 = 2$. All dimensionful quantities are given in units of m.*

be determined by integrating the evolution equation (2.3) numerically, or by using the approximate solution of eq. (2.4).

The various steps in our calculation are summarized in fig. 1, for two models described by a potential $U_{k_0}(\phi)$ given by eq. (3.1). In the following we express all dimensionful quantities in terms of the arbitrary mass scale m. In the first row we present results for a theory with $\gamma/m^2 = -2$, $h/m^2 = 1/3$. In (a) we present the evolution of the potential $U_k(\phi)$ as the scale k is lowered. We always shift the metastable vacuum to $\phi = 0$. The solid line corresponds to $k_0/m = 2$, while the line with longest dashes (that has the smallest barrier height) corresponds to $k_f/m = 1.1$. At the scale k_f the negative curvature at the top of the barrier is slightly larger than $-k_f^2$. This is the point in the evolution of the potential where configurations that interpolate between the minima start becoming relevant in the functional integral that defines the coarse-grained potential [19]. For this reason, we stop the evolution at this point. We observe that, for low k, the absolute minimum of the potential settles at a non-zero value of ϕ. A significant barrier separates it from the metastable minimum at $\phi = 0$. The profile of the saddle point $\phi_b(r)$ is plotted in (b) in units of m for the same sequence of scales. We observe a variation of the value of the field ϕ in the center of the critical bubble for different k. This is reflected in the form of the quantity $W_k(r)$, defined in eq. (2.8c), which we plot in (c).

Our results for the nucleation rate are presented in (d). On the horizontal axis we give the values of $\ln(k/m)$. The dark diamonds correspond to the values of the action S_k of the saddle point at the scale k. The stars indicate the values of $\ln(A_k/m^3)$. We observe a logarithmic k dependence for both these quantities. The value of A_k is expected to decrease for smaller k, because k acts as the effective ultraviolet cutoff in the calculation of the fluctuation determinants in A_k. For smaller k,

6

fewer fluctuations with wavelengths above an increasing length scale $\sim 1/k$ contribute explicitly to the fluctuation determinants. The logarithmic dependence on k is the reflection of the logarithmic ultraviolet divergence of the unregularized prefactor in two dimensions. The dark squares in (d) give our results for $-\ln(I/m^3) = S_k - \ln(A_k/m^3)$. The logarithmic k dependence largely cancels between S_k and $\ln(A_k/m^3)$, so that $\ln(I/m^3)$ is almost constant. The small residual dependence on k can be used to estimate the contribution of the next order in the expansion around the saddle point. This contribution is expected to be smaller than $\ln(A_k/m^3)$. This behaviour confirms that the nucleation rate should be independent of the scale k that we introduced as a calculational tool.

In the second row we present the calculation of the nucleation rate for a model with a larger coupling $h/m^2 = 2$, and $\gamma/m^2 = -4.5$, $k_0/m = 2$, $k_f/m = 1.1$. We observe a more pronounced k dependence of the potential, saddle-point profile and function $W_k(r)$. The most important aspect of the comparison of the two models concerns the relative values of S_k and $\ln(A_k/m^3)$. For the first model, the contribution of the prefactor to the nucleation rate is much smaller than that of the action of the saddle point. The main role of the prefactor is to remove the logarithmic k dependence from I/m^3. For the second model, S_k and $\ln(A_k/m^3)$ are comparable. This indicates that the effects of fluctuations are enhanced. Moreover, the prefactor fails to cancel the k dependence of the saddle-point action. The reason is that the next order in the expansion around the saddle point is important and can no longer be neglected. This establishes the limit of validity of homogeneous nucleation theory [5] for two-dimensional systems, in agreement with the studies of refs. [9]–[11] in three dimensions.

4 Comparison with lattice studies

4.1 Matching the lattice theory

A main objective of this work is the comparison of our results with the lattice study of ref. [21]. This requires a precise definition of the form of the potential. We must make sure that we consider a theory identical to the one simulated on the lattice. As we cannot match exactly the bare parameters of the lattice action, it is more convenient to guarantee that the low energy renormalized theory is the same in our model and ref. [21]. In the latter work, through a redefinition of the field and the distance, the one-loop renormalized action (free energy rescaled with respect to the temperature) of the (2+1)-dimensional theory at high temperature is expressed as

$$S = \frac{1}{\theta} \int d^2\tilde{x} \left\{ -\frac{1}{2} \left(1 - \frac{\theta}{48\pi} \right) \tilde{\phi} \, \tilde{\partial}^2 \tilde{\phi} + \tilde{V}(\tilde{\phi}) + \frac{\theta}{8\pi} \left[\tilde{V}''(\tilde{\phi}) - \tilde{V}''(\tilde{\phi}) \ln \left(\tilde{V}''(\tilde{\phi}) \right) \right] \right\}, \qquad (4.2)$$

with

$$\tilde{V}(\tilde{\phi}) = \frac{1}{2}\tilde{\phi}^2 - \frac{1}{6}\tilde{\phi}^3 + \frac{1}{24}\lambda\tilde{\phi}^4. \qquad (4.3)$$

For $\lambda < 0$ the potential becomes unbounded from below, while for $\lambda = 1/3$ it has two equivalent minima. For this reason, we consider λ values in the interval $(0, 1/3)$. Higher-loop corrections are expected to be proportional to larger powers of $\theta/8\pi$. This implies that the theory that is simulated on the lattice corresponds to a renormalized action in the continuum given by eqs. (4.2), (4.3) only if θ is not much larger than 1. In the opposite case, the renormalized action cannot be determined perturbatively.

In our approach the theory is defined at some initial scale k_0 and the integration of evolution equations such as eq. (2.3) generates the low-energy structure. For $k = 0$ the effective average action of eq. (2.1) must be identified with the action of eq. (4.2). We neglect wavefunction renormalization effects, which can be seen from eq. (4.2) to be a good approximation for values of θ not much larger than 1. The form of the potential at some non-zero scale k can be inferred by demanding that the iterative solution of eq. (2.4) reproduces the potential of eq. (4.2) for $k = 0$. In particular, by choosing $k = k_1 = 0$ in eq. (2.4) and renaming k_0 as k we find

$$U_k(\phi) \approx V(\phi) + \frac{1}{8\pi}V''(\phi) - \frac{1}{8\pi} \left(k^2 + V''(\phi) \right) \ln \left(\frac{k^2 + V''(\phi)}{m^2} \right), \qquad (4.4)$$

where $V(\phi)$ is given by eq. (3.1) with

$$\frac{\gamma}{m^2} = -\sqrt{\theta}, \qquad \frac{h}{m^2} = \frac{1}{3}\,\theta\,\lambda. \tag{4.5}$$

In eq. (4.4) we have neglected terms $\sim (8\pi)^{-2}$ and terms $\sim (8\pi)^{-1}$ in the arguments of the logarithms. It is clear from the above that the dimensionless coupling that controls the validity of the perturbative expansion is $\theta\lambda/3$. For this reason, perturbation theory is expected to break down for $\theta \gtrsim 3/\lambda$.

In summary, eq. (4.4) is an approximate solution of the evolution equation (2.3) (at the first level of an iterative procedure) which is consistent with eq. (4.2) that determines the renormalized action of ref. [21]. The matching between the renormalized and the lattice actions is accurate only at the one-loop level (the region of validity of eq. (4.2)). The approximate solution of eq. (4.4), which results at the first level of the iterative procedure, has a similar region of applicability. Morever, this approximation is not valid for values of k that render negative the argument of the logarithm in the right-hand side of eq. (4.4), i.e. for $k^2 < \max\{-V''(\phi)\}$. This implies that eq. (4.2) is trustable only in the convex regions of the potential (for which $\tilde{V}''(\phi) > 0$) and should not be expected to lead to reliable predictions for the nucleation rate. This is in agreement with the conclusion of ref. [21] that the determination of the bubble-nucleation rate through the real part of eq. (4.2) does not lead to consistency with the lattice results. On the other hand, eq. (4.2) is perfectly valid in the convex regions of the potential, where it can be matched with eq. (4.4) for $k = 0$. In the following, for our predictions of the bubble-nucleation rates and the comparison with the lattice results, we rely on the approximate solution of eq. (4.4), instead of integrating eq. (2.3) numerically. The numerical solution, which is more accurate than eq. (4.4), does not offer increased precision in our comparison with the lattice data, as the determination of the renormalized theory is valid only at the one-loop level[1].

4.2 Comparison with the lattice results

In fig. 2 we present a comparison of results obtained through our method with the lattice results of fig. 1 of ref. [21]. For each of several values of λ we vary the parameter θ and determine the couplings γ, h according to eqs. (4.5). The coarse-grained potential is then given by eq. (4.4) for $k \geq k_f$. The diamonds denote the saddle-point action S_k. For every choice of λ, θ we determine S_k at two scales: $1.2\,k_f$ and $2\,k_f$. The light-grey region between the corresponding points gives an indication of the k dependence S_k. The bubble-nucleation rate $-\ln\left(I/m^3\right)$ is denoted by dark squares. The dark-grey region between the values obtained at $1.2\,k_f$ and $2\,k_f$ gives a good check of the convergence of the expansion around the saddle-point. If this region is thin, the prefactor is in general small and cancels the k dependence of the action. The dark circles denote the results for the nucleation rate from the lattice study of ref. [21]. The dashed straight lines correspond to the action of the saddle-point computed from the 'tree-level' potential of eq. (3.1).

For $\lambda = 0$ the potential of eq. (3.1) is unbounded from below and the procedure we outlined in the previous paragraphs for matching the theory simulated on the lattice may be problematic. However, one may consider these results as applying to the limit $\lambda \to 0$, so that no conceptual problems arise. The values of $-\ln(I/m^3)$ computed at $1.2\,k_f$ and $2\,k_f$ are equal to a very good approximation, which confirms the convergence of the expansion around the saddle-point and the reliability of the calculation. The k dependence of the saddle-point action is cancelled by the prefactor, so that the total nucleation rate is k independent. Moreover, the prefactor is always significantly smaller than the saddle-point action. The circles indicate the results of the lattice simulations of ref. [21]. The agreement with the lattice predictions is good. More specifically, it is clear that the contribution of the prefactor is crucial for the correct determination of the total bubble-nucleation rate. Similar conclusions can be drawn for $\lambda = 0.1$ and $\lambda = 0.2$.

For larger values of λ the lattice simulations have been performed only for θ significantly larger than 1. For smaller θ, nucleation events become too rare to be observable on the lattice. As we

---

[1]We also perform checks of the corrections arising from integrating the full evolution equation (2.3). These corrections are very small in the parameter region for which the expansion around the saddle point is convergent.
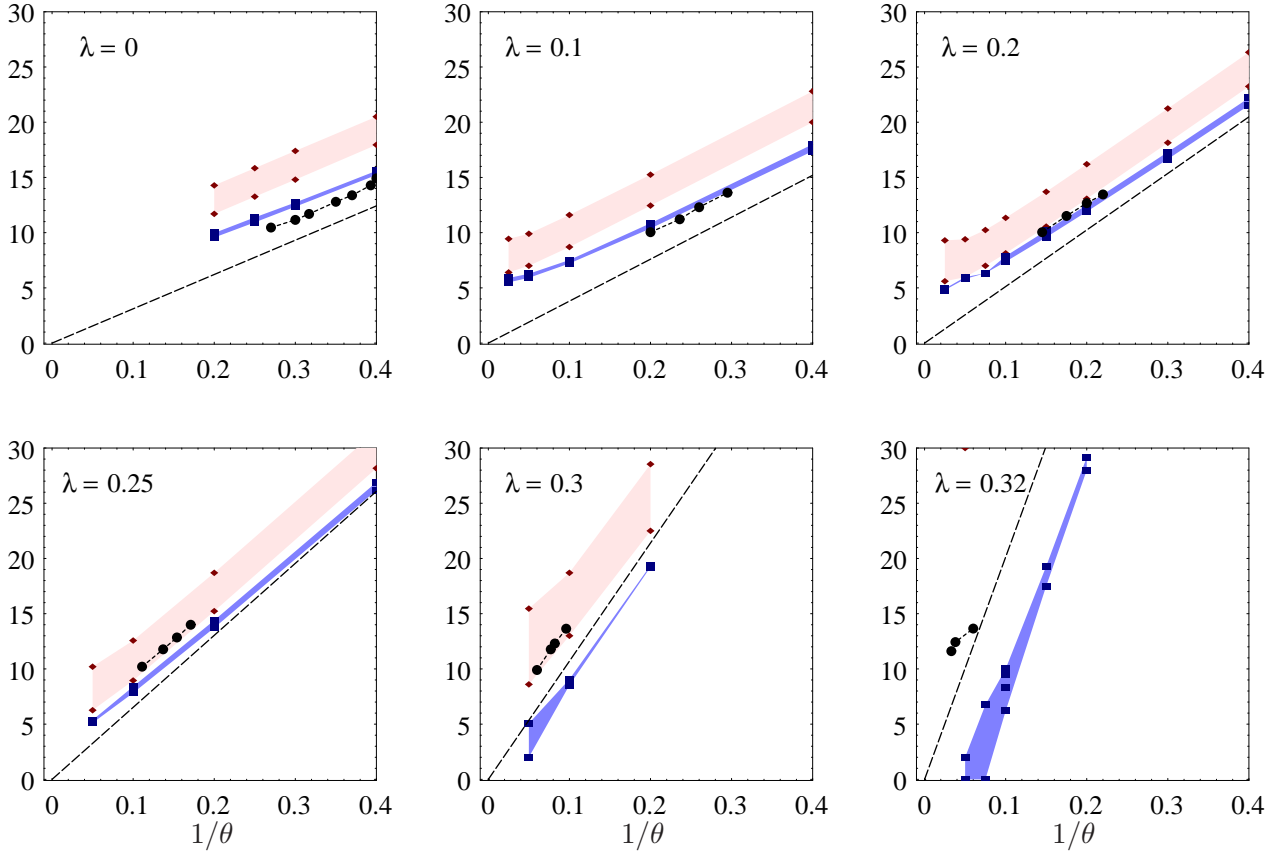
Figure 2: *Comparison of our method with lattice studies: Diamonds denote the saddle-point action S_k and squares the bubble-nucleation rate $-\ln\left(I/m^3\right)$ for $k = 1.2\,k_f$ and $2\,k_f$. Dark circles denote the results for the nucleation rate from the lattice study of ref. [21]. Finally, the dashed straight lines correspond to the action of the saddle-point computed from the potential of eq. (3.1).*

discussed earlier, the matching between the lattice and the renormalized actions becomes imprecise for large θ. This indicates that we should expect deviations of our results from the lattice ones, as the theory of eq. (4.2) may be different than the simulated one. These deviations start becoming apparent for the value $\lambda = 0.25$, for which the lattice simulations were performed with $\theta \sim 10$–20. For $\lambda \geq 0.3$ the lattice results are in a region in which the internal consistency criteria of our method for the reliability of the expansion around the saddle-point are not satisfied any more.

The consistency of our calculation is achieved for $1/\theta \gtrsim 0.12$ even for $\lambda = 0.32$. However, the breakdown of the expansion around the saddle point is apparent for $1/\theta \lesssim 0.12$. The k dependence of the predicted bubble-nucleation rate is strong[2]. The prefactor becomes comparable to the saddle-point action and the higher-order corrections are expected to be large. The k dependence of S_k is very large. For this reason we have not given values of S_k in this case. This behaviour indicates that the field fluctuations become significant. Typically, these fluctuations enhance the total rate and for $1/\theta \lesssim 0.08$ can even compensate the exponential suppression. Several similar examples were given in refs. [9]–[11].

The reason for this behaviour can be traced to the form of the differential operators in the prefactor (see eqs. eqs. (2.7)–(2.8c)). This prefactor, before regularization, involves the ratio $\det'(-\partial^2 + U_k''(0) + W_k(r))/\det(-\partial^2 + U_k''(0))$, with $W_k(r) = U_k''(\phi_b(r)) - U_k''(0)$. The function $W_k(r)$ always has a

---

[2]The additional squares for $1/\theta = 0.1$ correspond to results from the numerical integration of eq. (2.3).

minimum away from $r = 0$ (see figs. 1c and 1g), where it takes negative values. As a result the lowest eigenvalues of the operator $\det'(-\partial^2 + U_k''(0) + W_k(r))$ are smaller than those of $\det(-\partial^2 + U_k''(0))$. The elimination of the very large eigenvalues from the determinants through regularization does not affect this fact and the prefactor A_k is always larger than 1. Moreover, in cases such as those depicted in fig. 2f it becomes exponentially large because of the proliferation of low eigenvalues in $\det'(-\partial^2 + U_k''(0) + W_k(r))$. In physical terms, this implies the existence of a large class of field configurations of free energy comparable to that of the saddle-point. Despite the fact that they are not saddle points of the free energy (they are rather deformations of such a point) and are, therefore, unstable, they result in a dramatic increase of the nucleation rate. This picture is similar to that of "subcritical bubbles" of ref. [27]. In ref. [28] the nucleation rate was computed by first calculating a corrected potential that incorporates the effect of such non-perturbative configurations. The pre-exponential factor must be assumed to be of order 1 in this approach, as the effect of most deformations of the critical bubble has already been taken into account in the potential. In our approach the non-perturbative effects are incorporated through the prefactor. Both methods lead to similar conclusions for the enhancement of the total nucleation rate.

A final comment concerns the θ dependence of our results for the nucleation rate in fig. 2. For a given value of λ, we observe a linear dependence of $-\ln(I/m^3)$ on $1/\theta$ in the regions where the calculation is consistent. This is explained by the fact that the dominant θ dependence of the potential arises from the first term in the right-hand side of eq. (4.4). This is in agreement with the findings of ref. [21]. In the latter work, this linear dependence was not observed for $\lambda = 0.3$ and 0.32. The reason is that the range of θ used in the simulations was so large that the first term in the right-hand side of eq. (4.4) ceased to be dominant. Our results for small θ display the expected behaviour even for $\lambda = 0.32$.

5 Conclusions

In this paper we applied our approach for the calculation of bubble-nucleation rates to (2+1)-dimensional theories at non-zero temperature. We studied these theories at coarse-graining scales k below the temperature, where they display an effective two-dimensional behaviour. This provided the opportunity to check several points of our approach that depend on the dimensionality of the system. For example, the evolution equation for the coarse-grained potential has a different form than the one in the effective three-dimensional systems we studied in the past. Also, the pre-exponential factor in the bubble-nucleation rate has a logarithmic ultraviolet divergence before regularization, instead of the leading linear divergence in three dimensions. This divergence is reflected in the leading logarithmic dependence of the regularized prefactor on the scale k that acts as an ultraviolet cutoff (fig. 1). More crucially, the complementarity between the k dependence of the prefactor and the saddle-point action was observed again. This is a crucial point that guarantees that a physical quantity, such as the bubble-nucleation rate, is independent of the scale k that we introduced as a calculational tool. The validity of Langer's theory of homogeneous nucleation was confirmed, as long as the prefactor gave a contribution to the nucleation rate smaller than the leading exponential suppression by the action of the saddle point.

Another important aspect of this work concerns the comparison of our results with data from lattice simulations. This constitutes a stringent quantitative test of our method. We found good agreement between our results and the lattice data when the renormalized action for the theory that is simulated on the lattice is known (fig. 2). In these cases, we first match the renormalized action and then compute the nucleation rate. For part of the range of the lattice parameters this is not possible, because the renormalized action cannot be obtained from the lattice action perturbatively. However, the internal consistency criteria of our method provide a test of the reliability of our results in all cases.

References

[1] S. Coleman, Phys. Rev. D **15**, 2929 (1977).

[2] C.G. Callan and S. Coleman, Phys. Rev. D **16**, 1762 (1977).

[3] I. Affleck, Phys. Rev. Lett. **46**, 388 (1981).

[4] A.D. Linde, Nucl. Phys. B **216**, 421 (1983).

[5] J. Langer, Ann. Phys. **41**, 108 (1967); *ibid.* **54**, 258 (1969); Physica **73**, 61 (1974).

[6] P.A. Rikvold and B.M. Gorman, Ann. Rev. Comput. Phys. I, edited by D. Stauffer, (World Scientific, Singapore, 1994) p. 149.

[7] W.N. Cottingham, D. Kalafatis and R. Vinh Mau, Phys. Rev. B **48**, 6788 (1993); M. Gleiser, G.C. Marques and R.O. Ramos, Phys. Rev. D **48**, 1571 (1993); J. Baacke and V.G. Kiselev, Phys. Rev. D **48**, 5648 (1993); J. Baacke, *ibid.* **52**, 6760 (1995); J. Kripfganz, A. Laser and M.G. Schmidt, Nucl. Phys. B **433**, 467 (1995); G.H. Flores, R.O. Ramos and N.F. Svaiter, preprint hep-th/9903009.

[8] J. Berges, N. Tetradis and C. Wetterich, Phys. Lett. B **393**, 387 (1997); J. Berges and C. Wetterich, Nucl. Phys. B **487**, 675 (1997).

[9] A. Strumia and N. Tetradis, preprint SNS-PH/98-12, hep-ph/9806453.

[10] A. Strumia, N. Tetradis and C. Wetterich, preprint SNS-PH/98-13, hep-ph/9808263.

[11] A. Strumia and N. Tetradis, preprint SNS-PH/98-24, hep-ph/9811438.

[12] C. Wetterich, Nucl. Phys. B **352**, 529 (1991); Z. Phys. C **57**, 451 (1993); it ibid. **60**, 461 (1993).

[13] L.P. Kadanoff, Physics **2**, 263 (1966).

[14] C. Wetterich, Phys. Lett. B **301**, 90 (1993).

[15] K.G. Wilson, Phys. Rev. B **4**, 3174 and 3184 (1971); K.G. Wilson and I.G. Kogut, Phys. Rep. **12**, 75 (1974); F.J. Wegner, in: *Phase Transitions and Critical Phenomena*, vol. 6, eds. C. Domb and M.S. Green (Academic Press, New York, 1976).

[16] N. Tetradis and C. Wetterich, Nucl. Phys. B **422**, 541 (1994).

[17] T.R. Morris, Phys. Lett. B **329**, 241 (1994).

[18] N. Tetradis and C. Wetterich, Nucl. Phys. B **398**, 659 (1993); Int. J. Mod. Phys. A **9**, 4029 (1994); N. Tetradis, Nucl. Phys. B **488**, 92 (1997).

[19] A. Ringwald and C. Wetterich, Nucl. Phys. B **334**, 506 (1990); N. Tetradis and C. Wetterich, Nucl. Phys. B **383**, 197 (1992).

[20] M. Alford, H. Feldman and M. Gleiser, Phys. Rev. D **47**, 2168 (1993).

[21] M. Alford and M. Gleiser, Phys. Rev. D **48**, 2838 (1993).

[22] C. Wetterich, Mod. Phys. Lett. A **11**, 2573 (1996).

[23] J. Adams, J. Berges, S. Bornholdt, F. Freire, N. Tetradis and C. Wetterich, Mod. Phys. Lett. A **10**, 2367 (1995).

[24] W.H. Press, B.P. Flannery, S.A. Teukolsky and W.T. Vetterling, *Numerical Recipes: The Art of Scientific Computing* (University Press, Cambridge, 1988).

[25] S. Coleman, in *The Whys of Subnuclear Physics*, Proceedings of the International School, Erice, Italy, 1977, ed. by A. Zichichi, Subnuclear Series Vol. 15 (Plenum, New York, 1979).

[26] S. Wolfram, *The Mathematica book*, 3rd ed. (Wolfram Media/Cambridge University Press, 1996).

[27] M. Gleiser, E.W. Kolb and R. Watkins, Nucl. Phys. B **364**, 411 (1991); M. Gleiser and E.W. Kolb, Phys. Rev. Lett. **69**, 1304 (1992); Phys. Rev. D **48**, 1560 (1993); N. Tetradis, Z. Phys. C **57**, 331 (1993); G. Gelmini and M. Gleiser, Nucl. Phys. B **419**, 129 (1994); M. Gleiser, Phys. Rev. Lett. **73**, 3495 (1994); Phys. Rev. D **49**, 2978 (1994); E.J. Copeland, M. Gleiser and H.-R. Müller, Phys. Rev. D **52**, 1920 (1995); M. Gleiser, A. Heckler and E.W. Kolb, Phys. Lett. B **405**, 121 (1997); J. Borrill and M. Gleiser, Nucl. Phys. B **483**, 416 (1997).

[28] M. Gleiser and A.F. Heckler, Phys. Rev. Lett. **76**, 180 (1996).